

Accepted Manuscript

Photodegradation of sulfamethoxazole in environmental samples:
The role of pH, organic matter and salinity

Cindy Oliveira, Diana L.D. Lima, Carla Patrícia Silva, Vânia Calisto, Marta Otero, Valdemar I. Esteves



PII: S0048-9697(18)33199-1
DOI: doi:[10.1016/j.scitotenv.2018.08.235](https://doi.org/10.1016/j.scitotenv.2018.08.235)
Reference: STOTEN 28297
To appear in: *Science of the Total Environment*
Received date: 3 May 2018
Revised date: 2 August 2018
Accepted date: 18 August 2018

Please cite this article as: Cindy Oliveira, Diana L.D. Lima, Carla Patrícia Silva, Vânia Calisto, Marta Otero, Valdemar I. Esteves , Photodegradation of sulfamethoxazole in environmental samples: The role of pH, organic matter and salinity. Stoten (2018), doi:[10.1016/j.scitotenv.2018.08.235](https://doi.org/10.1016/j.scitotenv.2018.08.235)

This is a PDF file of an unedited manuscript that has been accepted for publication. As a service to our customers we are providing this early version of the manuscript. The manuscript will undergo copyediting, typesetting, and review of the resulting proof before it is published in its final form. Please note that during the production process errors may be discovered which could affect the content, and all legal disclaimers that apply to the journal pertain.

**Photodegradation of sulfamethoxazole in environmental samples: The
role of pH, organic matter and salinity**

Cindy Oliveira^a, Diana L.D. Lima^{b,c,*}, Carla Patrícia Silva^b, Vânia Calisto^b, Marta Otero^d,
Valdemar I. Esteves^b

^aDepartment of Chemistry, University of Aveiro, Campus de Santiago, 3810-193 Aveiro,
Portugal

^bCESAM & Department of Chemistry, University of Aveiro, Campus de Santiago, 3810-
193 Aveiro, Portugal

^cInstituto Politécnico de Coimbra, ESTESC-Coimbra Health School, Complementary
Sciences, Rua 5 de Outubro, S. Martinho do Bispo, 3046-854 Coimbra, Portugal

^dCESAM & Department of Environment and Planning, University of Aveiro, Campus de
Santiago, 3810-193 Aveiro, Portugal

* **corresponding author:** Dr. Diana L.D. Lima, CESAM & Department of Chemistry,

University of Aveiro, Campus de Santiago, 3810-193 Aveiro, Portugal. E-mail:

diana.lima@ua.pt. Tel.: +351 234 401 408. Fax: +351 234 370 084.

Abstract

Sulfamethoxazole (SMX) is the most representative antibiotic of the sulfonamides group used in both human and veterinary medicine, and thus frequently detected in water resources. Special concern is due to their pronounced toxicity and potential to foster bacterial resistance to this drug. Its photodegradation under simulated solar radiation was here studied in ultrapure water and in different environmental samples, namely estuarine water, freshwater and wastewater. SMX underwent very fast photodegradation in ultrapure water, presenting a half-life time ($t_{1/2}$) of 0.86 h. However, in environmental samples, the SMX photodegradation rate was much slower, with $5.4 \text{ h} < t_{1/2} < 7.8 \text{ h}$. The main novelty of this work was to prove that pH, salinity and dissolved organic matter are determinant factors in the decrease of the SMX photodegradation rate observed in environmental samples and, thus, they will influence the SMX fate and persistence, increasing the risks associated to the presence of this pollutant in the environment.

Keywords: Photolysis; sulfonamide antibiotics; apparent direct quantum yield; humic substances; emerging contaminants.

1. INTRODUCTION

In the aquatic environment, pharmaceuticals were detected for the first time in the 70's (Garrison et al., 1976). Since then, their presence in natural waters has been confirmed worldwide and they are actually recognized as contaminants of emerging concern (Yang et al., 2017).

The consumption of pharmaceuticals is rising with the growing and ageing of human population. Part of these pharmaceuticals is not metabolized and is released into sewage systems. However, conventional treatments applied in sewage treatment plants (STPs) do not adequately remove these pollutants from water. Therefore, pharmaceuticals are found in STP effluents and surface waters in concentrations ranging from ng L^{-1} to $\mu\text{g L}^{-1}$ (Bastos, 2012; Bila and Dezotti, 2003; Katsumata et al., 2014; Kümmerer, 2001). In the environment, these concentrations are high enough to affect non-target organisms (Challis et al., 2014).

The presence of pharmaceuticals in natural waters is especially concerning in the case of antibiotics, due to their pronounced toxicity and potential to foster bacterial resistance (Bila and Dezotti, 2003, Kümmerer, 2001). In a recent review on the monitoring of organic pollutants in surface and ground waters (Sousa et al., 2018), sulfamethoxazole (SMX) was pointed as the most reported antibiotic, as for its potential adverse effects on ecosystems and human health (Bastos, 2012, Avisar et al., 2009, Gastalho et al., 2014).

In the aquatic environment, photolysis, direct or indirect, is a major removal mechanism for many pharmaceuticals (Challis et al., 2014, Boreen et al., 2003). In the direct photolysis, light is absorbed directly by the chemical itself. In indirect photolysis, photosensitizers absorb the light generating photoreactants, such as OH radicals ($\cdot\text{OH}$)

or singlet oxygen ($^1\text{O}_2$) (Oliveira et al., 2016), that will interact with the pollutant, resulting in a chemical transformation. Also, among the reactive intermediates produced upon absorption of sunlight by surface waters, excited triplet states of chromophoric dissolved organic matter ($^3\text{CDOM}^*$) and carbonate radical ($\cdot\text{CO}_3^-$) play a major role in the indirect photodegradation of pollutants (McNeill and Canonica, 2016; Wallace et al., 2010). The direct and indirect photolysis of pharmaceuticals were among the issues recently evaluated by Challis et al. (2014) in their critical review of the scientific literature on the photodegradation of this sort of pollutants in the aquatic environment. In the specific case of SMX, and on the basis of published literature, these authors concluded that photolytic processes dominate its fate in the aquatic environment, direct photolysis is mostly pointed as the major mechanism while indirect photolysis is diversified between studies (Bonvin et al., 2013; Boreen et al., 2004; Challis et al., 2014; Lam and Mabury, 2005; Ryan et al., 2011; Wenk et al., 2011).

Different authors have evaluated the matrix effect that some environmental factors may have on the photodegradation of SMX. For example, Trovó et al. (2009) verified that, under simulated solar radiation, the SMX ($C_i = 10 \text{ mg L}^{-1}$) degradation was faster in distilled water ($\text{pH} = 4.8$) than in seawater ($\text{pH} = 8.1$). Niu et al. (2013) determined that the photodegradation of SMX ($C_i = 1, 5, 10 \text{ mg L}^{-1}$) under simulated sunlight irradiation was faster under lower pH values (between 3 and 10) and at lower concentration of SMX, fulvic acids and suspended sediments. Differently, Bahnmüller et al. (2014) observed that the transformation kinetics of SMX ($C_i = 1 - 5 \text{ }\mu\text{M}$, equivalent to $253 - 1265 \text{ }\mu\text{g L}^{-1}$) was not affected or just slightly ($< 20\%$) increased in the presence of fulvic acids as compared with ultrapure water.

As above shown, among the few works available in the literature on the influence of environmental factors on SMX photodegradation, either SMX concentrations used are rather high (in the mg L^{-1} range), or contradictory results were obtained. In this context, the aim of the present study was to further investigate the photodegradation of SMX ($C_i = 100 \mu\text{g L}^{-1}$) in real matrices (estuarine water, freshwater and wastewater samples) and to determine the role of pH, organic matter and salinity, which were considered the main factors that could affect the SMX photodegradation behaviour. Finally, the apparent quantum yields of photoreactions, as well as outdoor half-life times ($t_{1/2}$) of SMX at latitude 45°N were estimated.

2. MATERIAL AND METHODS

2.1. Chemicals

SMX (> 98%) and methanol (99.99%) were purchased from TCI (Europe) and Fisher Chemical, respectively. Ultrapure water was obtained from a Milli-Q Millipore system (Milli-Q plus 185). Acetonitrile (HPLC grade) and acetic acid (p.a.) used for HPLC analysis, were obtained from VWR (Prolabo) and Merck, respectively. The pH of solutions was adjusted using hydrochloric acid (NormaPur, 37%) and sodium hydroxide (ABSOLVE, 99.3%).

Sodium dihydrogen phosphate dihydrate (Fluka, Biochemika, $\geq 99.5\%$) and disodium hydrogen phosphate dihydrate (Fluka, Biochemika, $\geq 99\%$) were used to prepare a stock solution of phosphate buffer 0.1 mol L^{-1} . This was diluted to have a 0.001 mol L^{-1} phosphate buffer solution, which pH was adjusted to 5 and 7.3. Synthetic salt water (21‰) was prepared using *Red Sea Salt* (Red Sea Europe) in phosphate buffer solution (0.001 mol L^{-1}) with pH adjusted to 7.3. *Red Sea Salt* contains

biologically balanced, elevated levels of the elements: Calcium, Magnesium, Carbonates. Is free from synthetic additives and contains no nitrates, phosphates or heavy metals (Red Sea, 2018).

Calcium chloride dihydrate (p.a.) and magnesium chloride hexahydrate (p.a.) were provided by Merck and Riedel-de-Haën, respectively.

2.2. Instrumentation

A solar radiation simulator Solarbox 1500 (Co.fo.me.gra, Italy) was used for irradiation experiments. This instrument is equipped with a xenon arc lamp (1500 W) and UV filters that limit the transmission of light below 290 nm. All experiments were performed with a constant irradiation of 55 W m^{-2} (290–400 nm), which corresponds to 550 W m^{-2} in the spectral range, according to the manufacturer. The level of irradiance and temperature was monitored by a multimeter (Co.fo.me.gra, Italy) equipped with a UV 290–400 nm band sensor and a black standard temperature sensor. A parabolic reflection system was used to ensure irradiation uniformity in the chamber, which was kept refrigerated ($30 \pm 2 \text{ }^\circ\text{C}$) by an air cooling system.

A High-Performance Liquid Chromatograph Prominence system equipped with a fluorescence detector (HPLC-FLD) was used for the quantification of SMX. This HPLC-FLD unit includes a DGU-20A5R degasser, a CTO-20AC column oven, a LC-30AD pump and a SIL-30AC autosampler (all from Shimadzu).

2.3. Chromatographic analysis of SMX

A 100 mg L^{-1} SMX aqueous stock solution (methanol < 1%) was prepared and diluted with ultrapure water to have standards with concentrations ranging from 1 to

100 $\mu\text{g L}^{-1}$. For the HPLC separation, a Kinetex XB-C18 column (2.6 μm , 100 mm x 4.60 mm) was used. Cell and column temperature were kept constant at 25 $^{\circ}\text{C}$ and an injection volume of 20 μL was used. The mobile phase consisted of water (acidified with 1% acetic acid): acetonitrile (60:40 v/v) and the flow rate was maintained at 0.8 mL min^{-1} . Before use as mobile phase, acetonitrile and water with 1% of acetic acid were filtered through a 0.2 μm polyamide membrane filters (Whatman). SMX detection was performed with a fluorescence scanner prominence RF-20Axs from Shimadzu with an excitation wavelength of 265 nm and an emission wavelength of 343 nm.

2.4. Photodegradation experiments

2.4.1. Irradiation

Quartz tubes (1.8 cm internal diameter and 20 cm height) containing the aqueous sample or SMX solution were placed on a suitable support, brought inside the solar radiation simulator and subjected to irradiation. For each set of experiments, four quartz tubes capped with Parafilm M[®] were kept inside the solar simulator. One of the tubes was covered with aluminium foil to protect it from light (control).

Throughout irradiation experiments, 1000 μL aliquots were collected from each quartz tube at specified times (from 5 min of irradiation until no SMX was detected using HPLC-FLD) and analysed by HPLC-FLD for the concentration of SMX. The remaining concentration of SMX in irradiated solutions (C) was compared with that in the respective control (C_0) for determining the percentage of degradation at each irradiation time (t , h). Then, GraphPad Prism 5 was used to determine fittings of

experimental data to the pseudo first-order kinetic equation $C/C_0 = e^{-kt}$, where k is the pseudo first-order degradation rate constant (h^{-1}).

2.4.2. SMX photodegradation in ultrapure water and in environmental samples

Direct photodegradation of SMX was studied using a solution of $100 \mu\text{g L}^{-1}$ SMX (prepared by dilution of the stock solution), which was distributed into quartz tubes (20 mL in each tube) and irradiated as described in section 2.4.1.

Surface (estuarine and freshwater) and wastewater samples were used to study SMX indirect photodegradation in dissolved organic matter (DOM) rich matrices. Immediately after collection, all samples were filtered through $0.45 \mu\text{m}$ nitrocellulose membrane filters (Millipore) and stored at 4°C until use, within 7 days. The estuarine sample was collected from *Ria de Aveiro* (Aveiro, Portugal), at an urban location. The freshwater sample was collected from a river located in the same region. Finally, wastewater was sampled from one of the Aveiro's STPs, after secondary treatment, corresponding to the final effluent (STPF). These samples were characterized by UV-visible spectrometry, salinity, DOC, conductivity and pH (detailed information is presented in SM).

All samples were spiked with SMX to obtain a $100 \mu\text{g L}^{-1}$ concentration, distributed into quartz tubes and irradiated as described in section 2.4.1.

2.4.3. SMX photodegradation at different pH values

To study the pH influence on SMX photodegradation, solutions of SMX ($100 \mu\text{g L}^{-1}$) were prepared in a 0.001 mol L^{-1} phosphate buffer with pH adjusted to 5.0, 6.3 and 7.3. Irradiation experiments, as described in section 2.4.1., were carried out. Then,

freshwater samples ($100 \mu\text{g L}^{-1}$ SMX) with no pH adjustment (pH 7.3) and with pH adjusted to 6.3 were irradiated.

2.4.4. SMX photodegradation in the presence of humic substances

To study the influence of organic matter on SMX photodegradation, three fractions of humic substances (HS) were used: humic acids (HA), fluvic acids (FA) and XAD-4. These were extracted and isolated from estuarine water (collected at *Ria de Aveiro* (Aveiro, Portugal)) as described by Santos et al. (1994) and Esteves et al. (1995). The purified fractions of HS were characterized by elemental analysis, solid-state ^{13}C cross polarization magic angle spinning nuclear magnetic resonance (CPMAS-NMR), dissolved organic carbon content and UV-visible spectrophotometry, using the procedures described in Esteves et al. (2009).

SMX solutions ($100 \mu\text{g L}^{-1}$) in presence of each of the three HS fractions (HA, FA and XAD-4) at a concentration of 20 mg L^{-1} prepared in 0.001 mol L^{-1} phosphate buffer with pH 5.0 and 7.3 were irradiated for 1 h.

2.4.5. Effect of sea salts and inorganic ions on SMX photodegradation

The effect of sea salts was evaluated by irradiating for 5 hours solutions of SMX ($100 \mu\text{g L}^{-1}$) prepared in 0.001 mol L^{-1} phosphate buffer with pH adjusted to 7.3 and containing 21‰ NaCl or 21‰ sea salts (synthetic salt water from *Red Sea Salts*).

SMX photodegradation kinetics in these solutions were also determined and compared with those of the estuarine sample (pH 7.3) and ultrapure water with phosphate buffer at pH 7.3, both containing $100 \mu\text{g L}^{-1}$ SMX.

Since calcium and magnesium are two of the main constituents of salt water, 100 $\mu\text{g L}^{-1}$ SMX solutions prepared in 0.001 mol L^{-1} phosphate buffer with pH adjusted to 7.3 and containing 785 mg L^{-1} of magnesium or 261 mg L^{-1} of calcium were also irradiated for 5 hours and analysed with HPLC-FLD. Results were compared with those obtained using the estuarine water sample (pH 7.3) and ultrapure water with phosphate buffer at pH 7.3, both containing 100 $\mu\text{g L}^{-1}$ SMX. The magnesium and calcium concentrations chosen were similar to those of the *Red Sea Salts* mentioned previously.

2.5. Estimation of apparent direct quantum yields of SMX

The quantum yield of SMX (ϕ_{SMX}) is defined as the ratio between the SMX photodegradation rate and the rate of light absorption and was estimated by radiometry using the method described by Calisto et al. (2011). Briefly, for this purpose, the photon flux emitted by the light source was determined considering the measured overall lamp irradiance using a calibrated radiometer and the lamp emission intensity at each wavelength (as given by the manufacturer lamp spectrum). The lamp irradiance was subsequently converted into number of photons emitted by the lamp, per unit of sample volume and per unit of time, as described below.

The apparent direct quantum yield, (ϕ_{ave}), was estimated by equation 1:

$$\phi_{\text{ave}} = \frac{C_i \times k}{\sum I_{\lambda i}^0 \times (1 - 10^{-\epsilon_{\lambda i} \times b \times C_0}) \times \Delta\lambda} \quad (\text{Eq. 1})$$

where k is the pseudo first-order degradation rate constant (s^{-1}), C_i is the initial concentration of SMX in the solution (mol L^{-1}), $I_{\lambda i}^0$ is the lamp emission intensity at the

wavelength λ_i ($\text{Ein L}^{-1} \text{s}^{-1} \text{nm}^{-1}$), ε_{λ_i} is the molar absorptivity of the SMX at the wavelength λ_i ($\text{L mol}^{-1} \text{cm}^{-1}$), b is the path length inside the photoreactor (cm, corresponding to the internal diameter of the quartz cylindrical reactors) and $\Delta\lambda$ is the wavelength interval of acquisition of the spectral irradiance of the lamp (nm). Considering the experimental impossibility of determining the rate constant of a photodegradation process corresponding to the absorption of a single wavelength (for polychromatic light sources), the apparent direct quantum yield was determined for an overall average over the lamp emission wavelength. Thus, the SMX's apparent direct quantum yield (ϕ_{ave}) was calculated considering the lamp emission wavelength range (290–800 nm) and respective emission intensities for the irradiance level used during the experiments (55 W m^{-2} , 290–800 nm). The calculation of ϕ_{SMX} was performed considering that the diameter of the quartz tubes (cylindrical photoreactors) was 1.8 cm, the volume of irradiated solution was 20 mL and the solution exposure area was 36 cm^2 .

3. RESULTS AND DISCUSSION

3.1. SMX photodegradation in ultrapure water and in environmental water samples

The SMX photodegradation in ultrapure water is shown in Figure 1 [(C/C_0) versus time].

FIGURE 1

Complete photodegradation of SMX in ultrapure water occurred within 3 hours and followed a pseudo first-order kinetic model with rate constant (k_{meas}) of $0.81 \pm 0.04 \text{ h}^{-1}$ (Table 1). The absence of microbiological or thermal degradation was verified

by the controls. Also, methanol in the SMX working solutions (<0.001%) was proved to have neglectable effects.

TABLE 1

Data on the photodegradation of SMX in the environmental water samples are presented on Table 1 and the corresponding fittings to the pseudo first-order kinetic equation in Figure 1. The salinity, conductivity, DOC and pH (Table 2) of the environmental water samples used in this study were determined as specified in supplementary data. Meanwhile, UV-visible spectra of environmental samples are shown in Figure S1.

TABLE 2

There is an obvious decrease in the photodegradation rate of SMX in environmental water samples, when compared with ultrapure water. The $t_{1/2}$ (calculated as $\ln 2/k_{meas}$) obtained in ultrapure water (pH = 6.3) was lower than 1 h, while in estuarine and riverine water was around 5 h and in STPF it reached almost 8 h (Table 1). The $t_{1/2}$ times are strictly related to experimental conditions, but, assuming that the lamp properly simulates sunlight, results can be converted into outdoor $t_{1/2}$, in summer sunny days (SSD) equivalents (Table 1). Considering that the total energy reaching the ground on a sunny summer day (45°N latitude) is $7.5 \times 10^5 \text{ J m}^{-2}$, one summer sunny day (24 h day/night cycle) corresponds to 3.8 h of irradiation with the used equipment (Calisto et al., 2011). This conversion allows determining $t_{1/2}$ values in environmentally relevant conditions. In ultrapure water 0.23 SSD are needed to reach $t_{1/2}$. Meanwhile, in the environmental samples, the outdoor $t_{1/2}$ varied between 1.4 and 2.05 SSD. This means that, in the aquatic environment, photodegradation of SMX is much slower, increasing its environmental accumulation and persistence, along with

potential risks, such as enhancing microbial resistance through prolonged exposure of microorganisms to SMX. Thus, it is important to understand which are the main contributors to the photodegradation rate decrease.

3.2. Influence of pH on SMX photodegradation

The pH of the environmental samples varied between 7.2 and 8.1 (Table 2). The photodegradation rate constant depends upon the quantity of photons absorbed by each mole of SMX per unit of time and on the quantum yield. Then, since pH greatly affects the SMX speciation in solution and thus its UV-visible absorbance (Dias et al., 2014), photodegradation behaviour may be expected to vary depending on pH.

SMX has two pK_a values (1.85 and 5.60) and its chemical speciation changes with pH according to Figure S2. Since the molar ratio between SMX species is related to pH (Figure S3), at pH 1.0, around 88% of SMX is protonated, while at pH 4.0 almost 97% is in the neutral form. Within the pH range of the environmental samples here used (> 7) more than 96.2% of SMX is in the negative form.

In Figure 2 the kinetic curves of SMX photodegradation in ultrapure water (Figure 2 (a)) and in estuarine water (Figure 2 (b)) at different pH values are presented.

FIGURE 2

Bahnmüller et al. (2014) observed that the effect of pH on the photodegradation of SMX was irrelevant for values between 7.9 and 8.7. It is necessary to consider that in the referred pH range (7.9 – 8.7), SMX is in its negative form (Figure S2). However, in this work, by the analysis of Figure 2 and Table 1 it is evident the great influence of pH on SMX photodegradation within $5.0 < \text{pH} < 7.3$ (where the ratio between the negative

and the neutral forms of SMX increases with pH). For example, after 1 hour of irradiation, the photodegradation of SMX in ultrapure water at pH 7.3 was 35%. However, after the same time of irradiation, photodegradation in ultrapure water at pH 6.3 and pH 5.0 were 58% and 78%, respectively. These results showed that the direct photodegradation of SMX in ultrapure water is more efficient at pH 5.0 than at pH 6.3 and 7.3. This is further confirmed by the corresponding values of $t_{1/2}$ (Table 1) which were 0.49, 0.86 and 2.9 h, at pH 5.0, 6.3 and 7.3, respectively.

Figure 2 (b) shows that SMX photodegradation in estuarine water sample at pH 6.3 was almost complete after 8 h irradiation, while 22 h were necessary at pH 7.3. Analyzing ϕ_{ave} (Table 1), the highest value was obtained in ultrapure water at pH 5.0, while the lowest value corresponded to ultrapure water at pH 7.3. This agrees with the above referred effect of pH and with the highest absorption of UV radiation, for wavelengths between 290 and 310 nm by SMX in ultrapure water at pH 5.0 (Figure S4). Moreover, in Figure S4 it may be observed that, the lowest absorbance at 290 nm occurred at pH 8.0. This is also in agreement with the fact that the lowest SMX photodegradation rate in this work (Table 1) occurred in STPF, which had the highest pH (pH 8.0).

3.3. Influence of HS on SMX photodegradation

DOC analysis (Table 2) indicated that the STPF sample had the greatest content of organic carbon (26.45 mg L⁻¹), when compared with estuarine water (5.5 mg L⁻¹) and freshwater (3.14 mg L⁻¹). With respect to the UV-visible spectra of environmental samples, which are depicted in Figure S1, larger absorbance values are most likely caused by higher chromophore concentrations. Within this wavelength range,

absorbance values determined for STPF were higher than for freshwater and estuarine water. Therefore, a higher inner filter effect may be ascribed to the STPF sample, being responsible for the lower SMX degradation rate observed in this sample (Table 1).

The results on the photodegradation of SMX under the presence of HA, FA and XAD-4 after 1 h of irradiation are shown in Figure 3, where the photodegradation rate ($[1-(C/C_0)] \times 100\%$) is presented for each irradiated solution.

FIGURE 3

It is well known that organic matter, such as HS, can have photosensitizing or inhibitory effects (such as inner filter effect), which are antagonistic. The increase in the photodegradation rate is due to the photosensitizing properties of the organic matter, since it can be promoted to a transient excited state in which it may react with oxygen present in solution, forming reactive species, or react directly with organic compounds, promoting an enhancement in the photodegradation rate. On the other hand, DOM may also play an opposite role, decreasing the photodegradation rate, by three distinct effects: the inner filter effect (reducing the available energy for the target organic molecules present in solution), scavenging/quenching of reactive species, and inhibitor for the triplet-induced transformation of aquatic contaminants, by back-reductions to the parent compound by $^3\text{CDOM}^*$. The net effect is obtained by the balance of these opposite contributions (Andreozzi et al., 2003; Canonica and Laubscher, 2008; Wenk et al., 2011).

After analyzing the results, it is possible to conclude that the photodegradation of SMX in ultrapure water after 1 hour of irradiation is much higher than in the presence of any of the HS fractions at both the pH values tested (5.0 and 7.3). Thus, in the photodegradation of SMX under the experimental conditions here used, the inhibitory

effect of HS is higher than the photosensitizing capacity. Wenk et al. (2011) also observed a marked inhibition by DOM of triplet-induced oxidation for SMX. Compounds containing amine moieties, such as sulfonamides were mentioned as significantly affected by this inhibition process (Wenk and Canonica, 2012).

Results suggest an inverse correlation between the HS aromaticity and their photosensitizing effect, which is coincident with the observations of Oliveira et al. (2016), Calisto et al. (2011) and Silva et al. (2016). In this work, HS characterization (reported in the section C of SM) indicated that HA, for which the smallest SMX photodegradation percentage occurred, is the most hydrophobic fraction, more enriched in aromatic and/or chromophoric groups. Meanwhile, the contrary was observed for the XAD-4 fraction, which, as suggested by its lower carbon but higher oxygen content than HA and FA, was the richest fraction in oxygen functional groups (Table S3 of SM). On the other hand, the spectra of the three fractions of HS (Figure S5 of SM) show that, within the studied wavelength range, the absorbance followed the order $XAD-4 < FA < HA$. Therefore, the fact that HA present a higher ability to absorb radiation may explain, at least partially, the lower SMX photodegradation in their presence, as compared with FA and XAD-4. Also, a correlation has been mentioned between the aromatic degree of the DOM and the antioxidant activity. DOM of terrestrial origin with high aromaticity was shown to be a better inhibitor than DOM of aquatic origin with low aromaticity (Wenk and Canonica, 2012), and thus more likely to act as antioxidant.

Overall, the presence of DOM, as simulated by HS, has an inhibitory effect on the photodegradation of SMX, which corroborates the results obtained with environmental water samples.

3.4. Effect of sea salts and inorganic ions on SMX photodegradation

Riverine, STPF and estuarine water samples used in this study had values of salinity of 0, 2.0 and 20.8 ‰ (Table 2), respectively. Salinity, which has been shown to have an inhibitory effect on the photocatalytic degradation of sulfonamide antibiotics (Yang et al., 2015), may be underneath the lower first order rate constant here obtained in estuarine water as compared with ultrapure water (Table 1). The salinity of sea water is essentially a measure of the concentration of nine major elements (Cl, Na, Mg, Ca, K, Br, Sr, B and F) and two radicals (SO_4^- and HCO_3^-), which also dominate the composition of estuarine water (Head, 1985). Elements present in estuarine waters at less than 1 mg kg^{-1} , are usually referred as minor elements and, unlike the major elements, their concentration often varies considerable temporally and spatially (Head, 1985). Therefore, and given the impossibility of studying the effects of all elements, in this work, the main major elements were selected to study their effects on the photodegradation of SMX. For this purpose, the influence of sodium chloride, magnesium and calcium in SMX photodegradation was evaluated after 5 h of irradiation and compared with results obtained in ultrapure, synthetic salt water and estuarine water samples (Figure 4).

FIGURE 4

From the analysis of Figure 4, it is possible to verify that under the presence of Mg^{2+} , Ca^{2+} and NaCl, the photodegradation of SMX after 5 hours of irradiation was lower than in ultrapure water. As mentioned before, indirect photolysis consists of light absorption by photosensitizers, which generates many photoreactants, such as OH radicals ($\cdot\text{OH}$) or singlet oxygen ($^1\text{O}_2$). In fact, hydroxyl radicals were considered as

main contributors to the indirect photodegradation of SMX (Trovó et al., 2009). Contrarily, it has also been referred that some ions, such as chloride and bromide, can scavenge the hydroxyl radicals (Cheng et al., 2018; Umar and Aziz, 2013; Zhou et al., 2015), reducing the photodegradation of organic pollutants. Also, the possibility of SMX stabilization through complexation with metal ions should not be dismissed. Quivet et al. (2006) referred that the complexation with metal ions has an important influence in stabilization, which may explain the decrease of organic pollutants photodegradation.

In this work, magnesium was the cation whose presence most decreased the photodegradation of SMX as compared with ultrapure water (from 66% to 37%). The effect of calcium was not so pronounced. To find out if the decrease of SMX photodegradation could be related with complexation of SMX with Mg^{2+} and Ca^{2+} , the 3D fluorescence spectra (Figure S6) and UV-visible absorbance (Figure S7) of SMX were obtained in ultrapure water and in the presence of these cations. A reduction in SMX fluoresce intensity (Figure S6) and UV-visible absorbance (Figure S7) was observed in the presence of Mg^{2+} and Ca^{2+} , as well as the formation of a new fluorescence band in the presence of Mg^{2+} , which point to the possible complexation of SMX with these two cations.

As shown in Figure 4, the photodegradation of SMX after 5 h of irradiation in synthetic salt water (21‰ of sea salts) was about 50% lower than in ultrapure water, but similar to 21‰ of NaCl (50%) and estuarine water sample (53%).

To further investigate the influence of sea salts, SMX photodegradation ($100 \mu\text{g L}^{-1}$) in NaCl (21‰) and in synthetic salt water (21‰ sea salts) solutions with phosphate buffer (0.001 mol L^{-1}) at pH 7.3 were irradiated throughout time until SMX was not

detected. These results (Figure 5) evidenced a significant decrease in the SMX photodegradation rate in NaCl (21‰) and synthetic salt water (21‰ sea salts) when compared to ultrapure water. Moreover, as may be observed in Figure 5, SMX photodegradation kinetics in NaCl (21‰), synthetic salt water (21‰ sea salts) and estuarine water sample were very similar.

FIGURE 5

Fitted parameters of the pseudo first-order kinetic equation corresponding to the results in Figure 5, which are depicted in Table 1, confirmed the above observations. For ultrapure water (pH 7.3), a first order rate constant of $0.24 \pm 0.01 \text{ h}^{-1}$ was determined, which is higher than in the estuarine water sample ($0.13 \pm 0.01 \text{ h}^{-1}$), in the synthetic salt water ($0.133 \pm 0.003 \text{ h}^{-1}$) and in the NaCl solution ($0.143 \pm 0.004 \text{ h}^{-1}$), the latter three also at pH 7.3. These results confirmed that, under the presence of salts, photodegradation of SMX slows down, which in this work resulted in much higher SMX $t_{1/2}$ and lower ϕ when compared to ultrapure water (Table 1). On the other hand, the fitted k_{meas} and $t_{1/2}$ values obtained for the samples with the same salinity (21‰) were quite similar, which may be related to the presence of Na^+ and Cl^- .

3.5. Comparison with published results and future studies

In this work, an evident decrease, in the photodegradation rate of SMX in estuarine, riverine and STPF water samples as compared with ultrapure water, was observed. Differently, Bahnmüller et al. (2014) observed that, although SMX photodegradation in riverine water was similar to that in ultrapure water, a significantly higher photodegradation rate occurred in wastewater. This was related with the presence of photogenerated hydroxyl radical or by excited triplet states of

DOM, as previously proposed by Ryan et al. (2011) to explain the enhanced photodegradation of SMX in wastewater. However, these authors (Ryan et al., 2011) confirmed that SMX photodegradation was identical in lake and ultrapure water (the latter buffered at pH=8), as previously found by Boreen et al. (2004). Many factors may be underneath the different SMX photodegradation results found in different environmental matrices. In this work, the effects of pH, salinity and DOM were assessed. It was found that the direct photodegradation of SMX was more efficient at pH 5.0 > 6.3 > 7.3 in ultrapure water and at pH 6.3 > 7.3 in estuarine water, which is in line with previous findings (Trovó et al., 2009; Niu et al., 2013). However, Bahnmüller et al. (2014) observed no effect for pH values between 7.9 and 8.7, this may be related to the fact that at these values SMX is mainly in its anionic form. In fact, Willach et al. (2018) recently showed that the photodegradation of the neutral SMX (dominant at 2 < pH < 6) was faster than that of the anionic form (dominant at pH > 6), results that are in agreement with the present work. Regarding salinity, Yang et al. (2015) highlighted its inhibitory effects in the photodegradation of sulfonamides. This finding is in agreement with results in this work, which evidenced that the photodegradation of SMX under the presence of Mg²⁺, Ca²⁺ and NaCl was lower than in ultrapure water. Moreover, SMX photodegradation kinetics in NaCl (21‰), synthetic salt water (21‰ sea salts) and estuarine water were very similar. With regards to DOM, it was simulated by estuarine HS in the present study, resulting (for the three fractions here considered: HA, FA, XAD-4) in a decrease of SMX photodegradation as compared with wastewater. Contrarily, Andreozzi et al. (2003) observed that HS acted as photosensitizers for SMX. However, as in this work, the dominance of DOM inhibitory (versus sensitizing) effects on the photodegradation of SMX has been observed in

other studies (Lam and Mabury, 2005; Niu et al., 2013). In fact, a marked inhibition by DOM of triplet-induced oxidation was observed for the photodegradation of SMX by Wenk et al. (2011), who also found larger inhibitory effect for DOM of terrestrial than on aquatic origin.

Overall, it is evident the complexity of SMX photodegradation in environmental matrices. In this study, it has been evidenced the important role of pH, organic matter and salinity. However, still there is much work to do and many other factors that should be considered in future works to further understand the behaviour of SMX in the aquatic environment. Such future works include, for example, to study: (i) the influence of the DOM concentration and origin, namely terrestrial or from different aquatic environments; (ii) the effects of nitrate, nitrite, carbonate, hydrogenocarbonate, sulfate, bromide, fluoride, iron, etc., and their concentrations on the photodegradation of SMX; or (iii) the effects of transient species generated under irradiation of the different photoactive species present in the aquatic environment. On the other hand, it has already been shown that the direct photolysis of SMX produces some metabolites that retain biological activity and that may retransform to the parent compound (Bonvin et al., 2013), which underlines the necessity of studying the photoproducts of SMX, their behaviour in environmental matrices and the role of environmental factors.

4. CONCLUSIONS

SMX photodegradation in environmental waters was observed to be lower than in ultrapure water. Therefore, the effects of pH, DOM, salinity and some inorganic ions were separately assessed. It was possible observed that SMX photodegradation

decreased with increasing pH between 5.0 and 8.0, which is related to changes in chemical speciation of SMX. On the other hand, DOM, simulated by humic substances (HS), resulted in the decrease of SMX photodegradation as for the inner filter effect of HS. Moreover, salinity also caused a decrease in the SMX photodegradation, either by the possible complexation of SMX with cations, or by the ability of anions, such as chloride, to scavenge the hydroxyl radicals responsible for indirect photodegradation.

Acknowledgements

This work was funded by FEDER through CENTRO 2020 and by national funds through FCT within the research project CENTRO-01-0145-FEDER-029021. Diana Lima and Vânia Calisto thank FCT for their post-doctoral grants (SFRH/BPD/80315/2011 and SFRH/BPD/78645/2011, respectively). Marta Otero thanks support by FCT Investigator Program (IF/00314/2015). Thanks are due, for the financial support to CESAM (UID/AMB/50017/2013), to FCT/MEC through national funds, and the co-funding by the FEDER, within the PT2020 Partnership Agreement and Compete 2020.

5. REFERENCES

- A.G. Trovó, R.F.P. Nogueira, A. Agüera, C. Sirtori, A.R. Fernández-Alba, Photodegradation of sulfamethoxazole in various aqueous media: Persistence, toxicity and photoproducts assessment. *Chemosphere* 77 (2009) 1292–1298.
- Andreozzi, R., Raffaele, M., Nicklas, P., 2003. Pharmaceuticals in STP effluents and their solar photodegradation in aquatic environment. *Chemosphere* 50, 1319–1330.
- Avisar, D., Lester, Y., Ronen, D., 2009. Sulfamethoxazole contamination of a deep phreatic aquifer. *Sci. Total Environ.* 407, 4278–4282.
- Bahn Müller, S., von Gunten, U., Canonica, S., 2014. Sunlight-induced transformation of sulfadiazine and sulfamethoxazole in surface waters and wastewater effluents. *Water Res.* 57, 183–192.
- Bastos, R.V., 2012. Estudo da degradação do antibiótico sulfametoxazol em solução aquosa por fotólise (Master's Thesis), University of São Paulo.
- Bila, D.M., Dezotti, M., 2003. Fármacos no meio ambiente. *Quim. Nova* 26, 523–530.
- Bonvin, F., Omlin, J., Rutler, R., Schweizer, W.B., Alaimo, P. J., Strathmann, T. J., McNeill, K., Kohn, T., 2013. Direct Photolysis of Human Metabolites of the Antibiotic Sulfamethoxazole: Evidence for Abiotic Back-Transformation. *Environ. Sci. Technol.* 47, 6746-6755.
- Boreen, A.L., Arnold, W.A., McNeill, K., 2003. Photodegradation of pharmaceuticals in the aquatic environment: A review. *Aquat. Sci.* 65, 320–341.
- Boreen, A.L., Arnold, W.A., McNeill, K., 2004. Photochemical Fate of Sulfa Drugs in the Aquatic Environment: Sulfa Drugs Containing Five-Membered Heterocyclic Groups. *Environ. Sci. Technol.* 38, 3933-3940.

- Calisto, V., Domingues, M.R.M., Esteves, V.I., 2011. Photodegradation of psychiatric pharmaceuticals in aquatic environments – Kinetics and photodegradation products. *Water Res.* 45, 6097–6106.
- Canonica, S., Laubscher, H.U., 2008. Inhibitory effect of dissolved organic matter on triplet-induced oxidation of aquatic contaminants. *Photochem. Photobiol. Sci.* 7, 547-551.
- Challis, J.K., Hanson, M.L., Friesen, K.J., Wong, C.S., 2014. A critical assessment of the photodegradation of pharmaceuticals in aquatic environments: defining our current understanding and identifying knowledge gaps. *Environ. Sci.-Proc. Imp.* 16, 672–696.
- Cheng, S., Zhang, X., Yang, X., Shang, C., Song, W., Fang, J., Pan, Y., 2018. The Multiple Role of Bromide Ion in PPCPs Degradation under UV/Chlorine Treatment. *Environ. Sci. Technol.* 52, 1806–1816.
- Dias, I.N., Souza, B.S., Pereira, J.H.O.S., Moreira, F.C., Dezotti, M., Boaventura, R.A.R., Vilar, V.J.P., 2014. Enhancement of the Photo-Fenton Reaction at Near Neutral pH Through the Use of Ferrioxalate Complexes: A Case Study on Trimethoprim and Sulfamethoxazole Antibiotics Removal from Aqueous Solutions. *Chem. Eng. J.* 247, 302–313.
- Esteves, V.I., Otero, M., Duarte, A.C., 2009. Comparative characterization of humic substances from the open ocean estuarine water and fresh water. *Org. Geochem.* 40, 942–950.
- Esteves, V.I., 1995. *Extracção e caracterização de substâncias húmicas de diferentes ambientes aquáticos (PhD thesis)*, Universidade de Aveiro.
- Garrison, A.W., Pope, J.D., Allen, F.R., 1976. Identification and Analysis of Organic Pollutants in Water, in Keith C. H. (Eds.), *GC/MS analysis of organic compounds in domestic wastewater*. Ann Arbor Science Publishers, Ann Arbor, pp. 517-556.
- Gastalho, S., Silva, G.J., Ramos, F., 2014. Antibiotics in aquaculture and bacterial resistance: Health care impact. *Acta Farmacêutica Portuguesa* 3, 29–45.

- Head, 1985. Salinity, dissolved oxygen and nutrients. In: Practical Estuarine Chemistry. A handbook. Ed. P.C. Head. Cambridge University Press, Cambridge, UK, pp. 94-125.
- Katsumata, C.P., Silva, M.P., Batista, A.P.S., Teixeira, A.C.S.C., 2014. Tratamento de água contaminada com fármacos por meio de fotólise UV e UV/H₂O₂, in XX Brazilian Congress of Chemical Engineering, pp. 1–8.
- Kümmerer, K., 2001. Drugs in the environment: Emission of drugs, diagnostic aids and disinfectants into wastewater by hospitals in relation to other sources - A review. *Chemosphere* 45, 957–969.
- Lam, M.W., Mabury, S.A., 2005. Photodegradation of the pharmaceuticals atorvastatin, carbamazepine, levofloxacin, and sulfamethoxazole in natural waters. *Aquat. Sci.* 67, 177-188.
- McNeill, K., Canonica, S., 2016. Triplet state dissolved organic matter in aquatic photochemistry: reaction mechanisms, substrate scope, and photophysical properties. *Environ. Sci.: Processes Impacts* 18, 1381-1399.
- Niu, J., Zhang, L., Li, Y., Zhao, J., Lv, S., Xiao, K., 2013. Effects of environmental factors on sulfamethoxazole photodegradation under simulated sunlight irradiation: Kinetics and mechanism. *J. Environ. Sci.* 25, 1098–1106.
- Oliveira, C., Lima, D.L.D., Silva, C.P., Otero, M., Esteves, V.I., 2016. Photodegradation behaviour of estriol: An insight on natural aquatic organic matter influence. *Chemosphere* 159, 545–551.
- Quivet, E., Faure, R., Georges, J., Paissé, J.-O., Lantéri, P., 2006. Influence of metal salts on the photodegradation of imazapyr, an imidazolinone pesticide. *Pest Manag. Sci.* 62, 407–413.
- Red Sea, 2018. Retrieved February, 2015, from www.redseafish.com/red-sea-salts/red-sea-salt/

- Ryan, C.C., Tan, D.T., Arnold, W.A., 2011. Direct and indirect photolysis of sulfamethoxazole and trimethoprim in wastewater treatment plant effluent. *Water Res.* 45, 1280-1286.
- Ryan, C.C., Tan, D.T., Arnold, W.A., 2011. Direct and indirect photolysis of sulfamethoxazole and trimethoprim in wastewater treatment plant effluent. *Water Res.* 45, 1280-1286.
- Santos, M.E., Esteves, V.I., Amado, F.L., Duarte, A.C., 1994. Humic Substances in the Global Environment and Implications on Human Health, in Senesi N., Miano T. M. (Eds.) Elsevier, Amsterdam, pp. 877-882.
- Silva, C.P., Lima, D.L.D., Otero, M., Esteves, V.I., 2016. Photosensitized Degradation of 17 β -estradiol and 17 α -ethinylestradiol: Role of Humic Substances Fractions. *J. Environ. Qual.* 45, 693–700.
- Sousa, J.C.G, Ribeira, A.R, Barbosa, M.O, Pereira, M.F.R, Silva, A.M.T., 2018. A review on environmental monitoring of water organic pollutants identified by EU guidelines. *J. Hazard. Mater.* 344, 146–162.
- Umar, M., Aziz, H.A., 2013. Photocatalytic Degradation of Organic Pollutants in Water, in Rashed N.M. (Eds), *Organic Pollutants - Monitoring Risk and Treatment*, InTech, pp. 195–207.
- Wallace, D.F., Hand, L.H., Oliver, R.G., 2012. The role of indirect photolysis in limiting the persistence of crop protection products in surface waters. *Environ. Toxicol. Chem.*, 29, 575–581.
- Wenk, J., Canonica, S., 2012. Phenolic Antioxidants Inhibit the Triplet-Induced Transformation of Anilines and Sulfonamide Antibiotics in Aqueous Solution. *Environ. Sci. Technol.* 46, 5455-5462.
- Wenk, J., von Gunten, U., Canonica, S., 2011. Effect of Dissolved Organic Matter on the Transformation of Contaminants Induced by Excited Triplet States and the Hydroxyl Radical. *Environ. Sci. Technol.* 45, 1334-1340.

- Willach, S., Lutze, H.V., Eckey, K., Löppenberg, K., Lüling, M., Wolbert, J.B., Kujawinski, D.M., Jochmann, M.A., Karst, U., Schmidt, T.C., 2018. Direct Photolysis of Sulfamethoxazole Using Various Irradiation Sources and Wavelength Ranges—Insights from Degradation Product Analysis and Compound-Specific Stable Isotope Analysis. *Environ. Sci. Technol.* 52, 1225-1233.
- Yang, C.-C., Huang, C.-L., Cheng, T.-C., Lai, H.-T., 2015. Inhibitory effect of salinity on the photocatalytic degradation of three sulfonamide antibiotics. *Int. Biodeter. Biodegr.* 102, 116–125.
- Yang, C.-C., Huang, C.-L., Cheng, T.-C., Lai, H.-T., 2015. Inhibitory effect of salinity on the photocatalytic degradation of three sulfonamide antibiotics. *Int. Biodeter. Biodegr.* 102, 116–125.
- Yang, Y., Ok, Y.S., Kim, K.-H, Kwon, E.E., Tsang, Y.F., 2017. Occurrences and removal of pharmaceuticals and personal care products (PPCPs) in drinking water and water/sewage treatment plants: A review. *Sci. Total Environ.* 596–597, 303–320.
- Zhou, L., Deng, H., Gao, Y., 2015. Photodegradation of sulfamethoxazole and photolysis active species in water under UV-Vis light irradiation. *Fresen. Environ. Bull.* 24, 1685–1691.

Figure 1. Kinetics of SMX photodegradation ($C_i = 100 \mu\text{g L}^{-1}$) in ultrapure water and in three different environmental aquatic matrices at natural pH values. Experimental results are shown together with curves of pseudo first-order decay fitted to the data by nonlinear regression. Shown error bars are standard deviations ($n = 3$) (note that, for the majority of the experimental points, error bars are so small that are not visible in the figure).

Figure 2. Experimental results on the kinetics of SMX photodegradation ($C_i = 100 \mu\text{g L}^{-1}$) together with curves of pseudo first-order decay fitted to the data by nonlinear regression obtained in (a) ultrapure water with phosphate buffer at different pH values; and in (b) estuarine water at different pH values. Shown error bars are standard deviations ($n = 3$) (note that, for the majority of the experimental points, error bars are so small that are not visible in the figure).

Figure 3. SMX photodegradation (%) in ultrapure water ($C_i = 100 \mu\text{g L}^{-1}$) and in presence of different HS fractions (20mg L^{-1}) prepared in phosphate buffer (0.001mol L^{-1}) at pH 5.0 and 7.3 after 1 hour of irradiation. Shown error bars are standard deviations ($n = 3$).

Figure 4. SMX photodegradation ($C_i = 100 \mu\text{g L}^{-1}$) in ultrapure water, in ultrapure water in the presence of Mg^{2+} , Ca^{2+} e NaCl , in synthetic salt water and in estuarine water, with phosphate buffer at pH 7.3 after 5 hours of irradiation. Shown error bars are standard deviations ($n=3$).

Figure 5. Kinetics of SMX photodegradation ($C_i = 100 \mu\text{g L}^{-1}$) in ultrapure water, in estuarine water, in synthetic saltwater and in a NaCl solution, all at pH 7.3 in presence of phosphate buffer. Experimental results are shown together with curves of pseudo first-order decay fitted to the data by nonlinear regression. Shown error bars are standard deviations ($n =$

3) (note that, for most the experimental points, error bars are so small that are not visible in the figure).

ACCEPTED MANUSCRIPT

Table 1. Data on pseudo first-order rate constants, k_{meas} , determination coefficient, R^2 , half-lives in simulated solar radiation, $t_{1/2}$ (h), half-lives in summer sunny days equivalents, $t_{1/2}$ (SSD), and apparent direct quantum yield (ϕ_{ave}).

ACCEPTED MANUSCRIPT

Table 1. Data on pseudo first-order rate constants, k_{meas} , determination coefficient, R^2 , half-lives in simulated solar radiation, $t_{1/2}$ (h), half-lives in summer sunny days equivalents, $t_{1/2}$ (SSD), and apparent quantum yield (ϕ_{ave}).

Sample	pH	$k_{\text{meas}} (\text{h}^{-1})^{\text{j}}$	R^2	$t_{1/2} (\text{h})^{\text{j}}$	$t_{1/2} (\text{SSD})^{\text{j}}$	ϕ_{ave}
Ultrapure water	5.0*	1.4 ± 0.1	0.9812	0.49 ± 0.04	0.13 ± 0.01	17.2×10^{-8}
Ultrapure water	6.3	0.81 ± 0.04	0.9900	0.86 ± 0.04	0.23 ± 0.01	2.76×10^{-8}
Ultrapure water	7.3*	0.24 ± 0.01	0.9767	2.9 ± 0.2	0.76 ± 0.05	2.42×10^{-8}
Estuarine water	6.3*	0.25 ± 0.02	0.9713	2.8 ± 0.2	0.74 ± 0.05	-----
Estuarine water	7.3	0.13 ± 0.01	0.9256	5.4 ± 0.5	1.4 ± 0.1	-----
Riverine water	7.2	0.117 ± 0.007	0.9701	5.9 ± 0.4	1.56 ± 0.09	-----
STPF	8.1	0.089 ± 0.002	0.9938	7.8 ± 0.2	2.05 ± 0.05	-----
Synthetic salt water (21‰)	7.3*	0.133 ± 0.003	0.9949	5.2 ± 0.1	1.37 ± 0.04	0.679×10^{-8}
NaCl (21‰)	7.3*	0.143 ± 0.004	0.9938	4.8 ± 0.1	1.27 ± 0.04	1.23×10^{-8}

*pH adjusted with HCl or NaOH; ^jAverage values are presented together with corresponding standard deviation.

Table 2 - Salinity, conductivity, dissolved organic carbon (DOC) and pH values of the samples tested.

Sample	Salinity (‰)	Conductivity ($\mu\text{S}/\text{m}$)	DOC (mg L^{-1})	pH
Estuarine water	20.8	24.00	5.5 ± 0.1	7.3
Riverine water	0	0.087	3.14 ± 0.07	7.2
STPF	2.0	2.820	26.45 ± 0.03	8.1

Figure 1

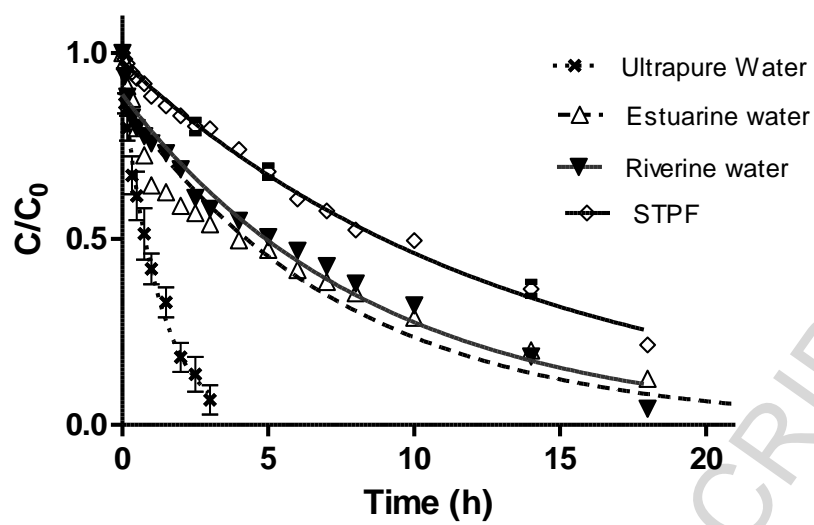


Figure 2

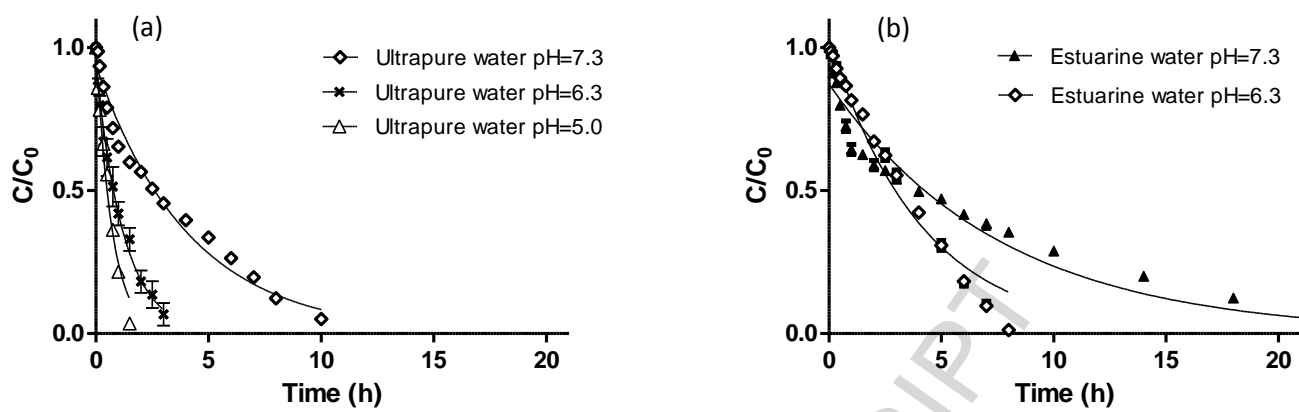


Figure 3

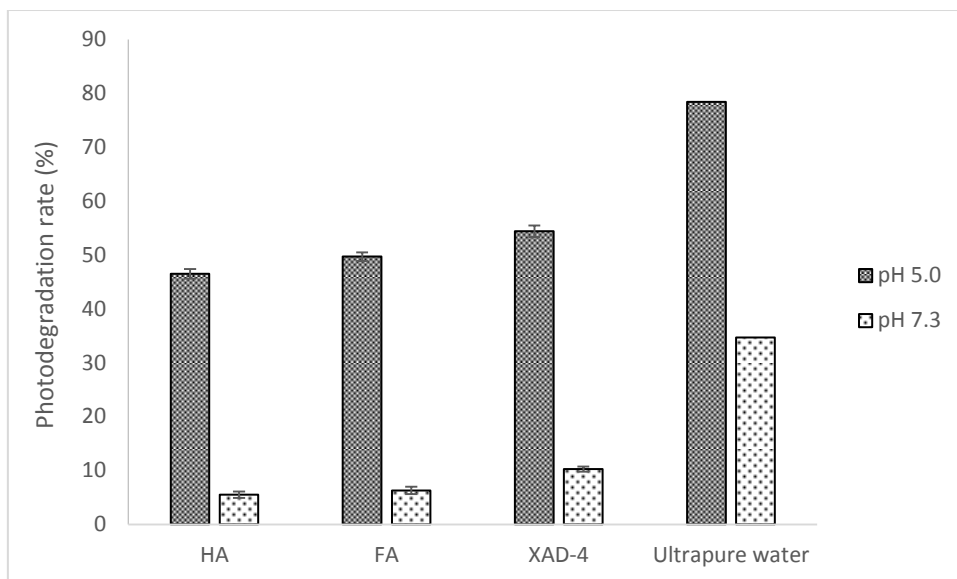


Figure 4

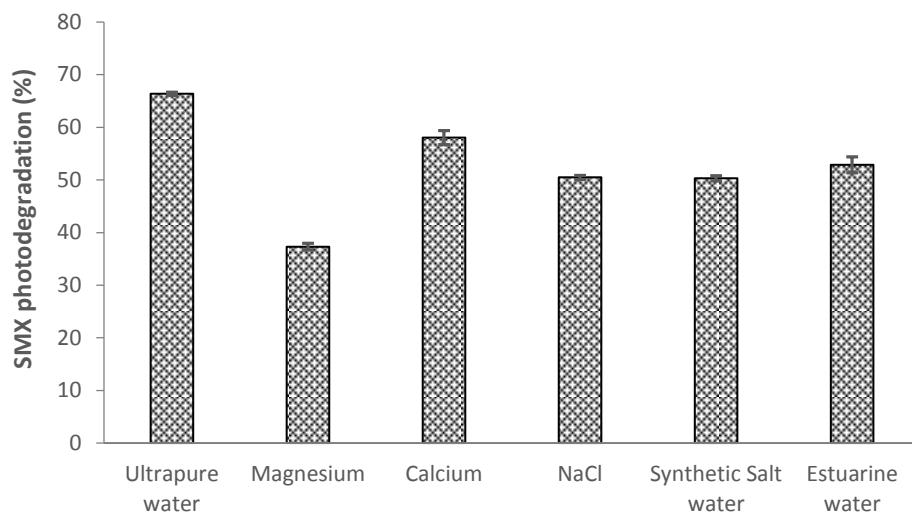
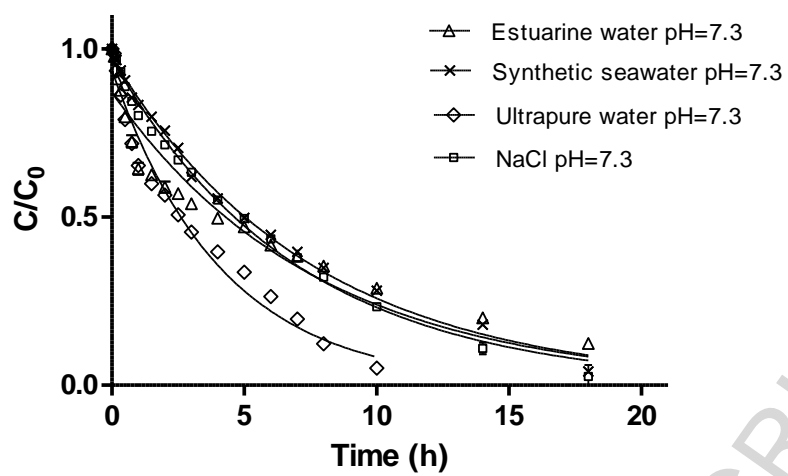
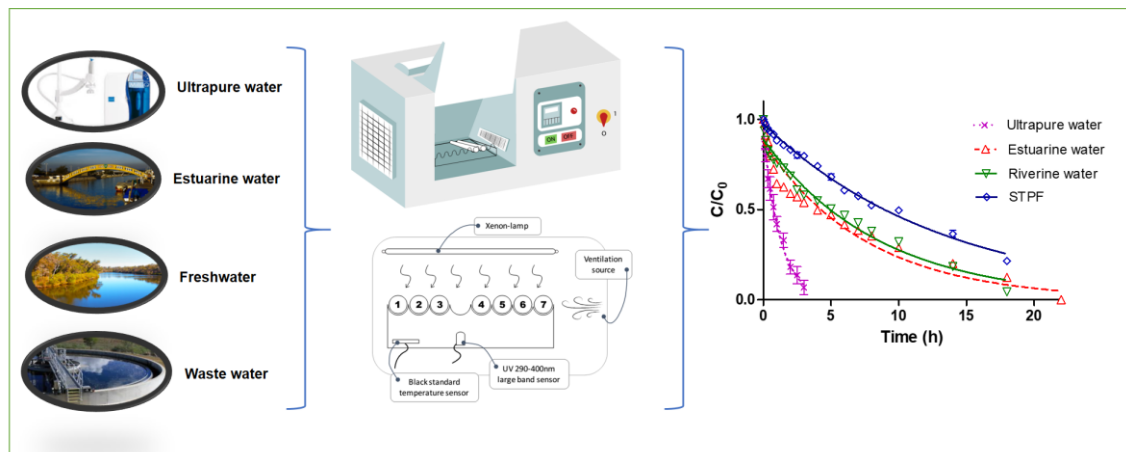


Figure 5





Graphical abstract

Highlights

- SMX underwent very fast photodegradation in ultrapure water
- $t_{1/2}$ increased from 0.86 h in ultrapure water to 5.4-7.8 h in environmental samples
- SMX photodegradation decreased with increasing pH of water samples
- Dissolved organic matter resulted in the decrease of SMX photodegradation
- Salinity also caused a decrease in the SMX photodegradation

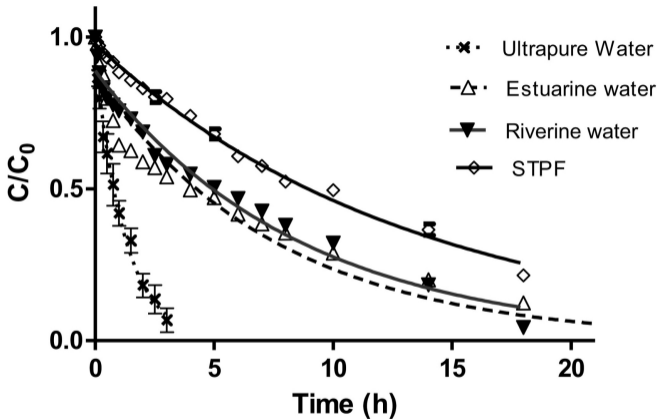


Figure 1

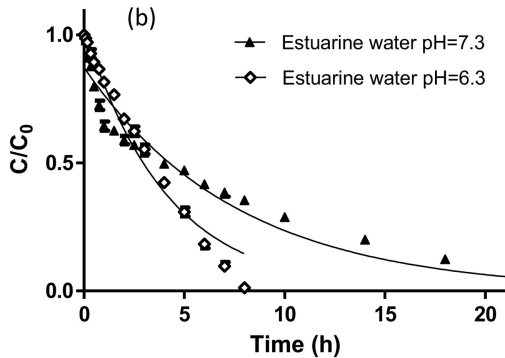
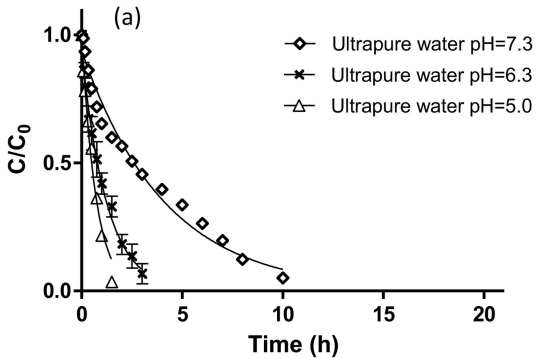


Figure 2

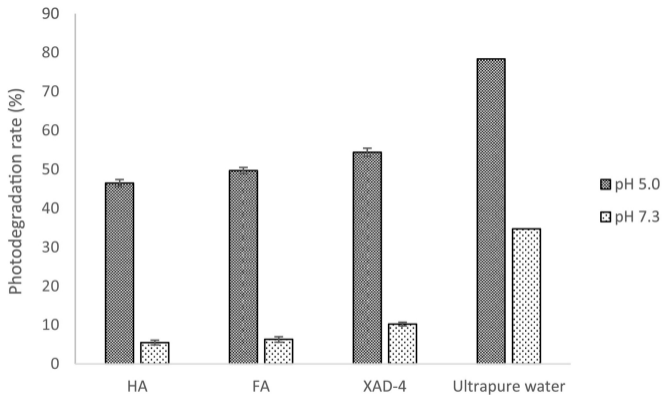


Figure 3

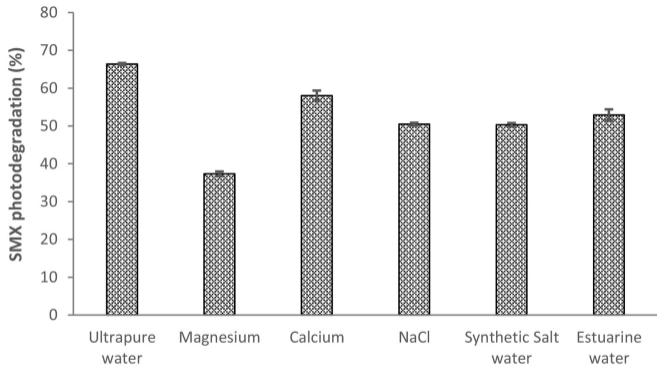


Figure 4

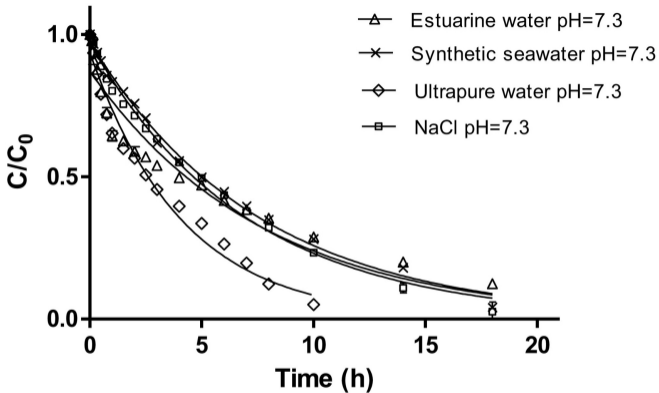


Figure 5